DOI:10.1021/jf100574j

JOURNAL OF AGRICULTURAL AND FOOD CHEMISTRY
ARTICLE

Oleanolic Acid and Ursolic Acid Induce Apoptosis in HuH7 Human Hepatocellular Carcinoma Cells through a Mitochondrial-Dependent Pathway and Downregulation of XIAP

Ming-Huan Shyu, Tzu-Chien Kao, and Gow-Chin Yen*

Department of Food Science and Biotechnology, National Chung Hsing University, 250 Kuokuang Road, Taiching 402, Taiwan

Oleanolic acid (OA) and ursolic acid (UA) are commonly found in plants and herbs and have been reported to possess hepatoprotective, anti-inflammatory and anticancer activities. In the present study, the effects of OA and UA on induction of apoptosis in human hepatocellular carcinoma HuH7 cells and the related mechanisms were investigated. The results demonstrate that OA and UA could inhibit the growth of HuH7 cells with IC_{50} values of 100 and 75 μM, respectively. Cell cycle analysis using flow cytometry indicated that the fraction of HuH7 cells in sub-G1 phase progressively increased with increasing concentrations of OA or UA from 20 to 80 μM. Treatment with OA and UA for 8 h induced a dramatic loss of the mitochondria membrane potential and interfered with the ratio of expression levels of pro- and antiapoptotic Bcl-2 family members in HuH7 cells. OA and UA-induced apoptosis involving the release of mitochondria cytochrome *c* into the cytosol and subsequently induced the activation of caspase-9 and caspase-3, followed by cleavage of poly (ADP-ribose) polymerase (PARP). Moreover, HuH7 cells treated with OA and UA suppressed the activity of NF-κB and modulated the mRNA expression of X-linked inhibitor of apoptotic protein (XIAP) as compared with untreated cells. These results demonstrate that OA and UA induce apoptosis in HuH7 cells through a mitochondria-mediated pathway and downregulation of XIAP.

KEYWORDS: HuH7 cell; apoptosis; oleanolic acid; ursolic acid and XIAP

INTRODUCTION

Ursolic acid (UA) and oleanolic acid (OA) are triterpenoid compounds found in plants, herbs and other foods. They are found in the free form or bound to glycosides (*1*). OA and UA have similar chemical structures but differ with respect to the position of a methyl group in the E loop; if the methyl group on C19 of UA is moved to C20, the compound becomes OA (**Figure 1**). UA and OA have been demonstrated to have anti-inflammatory, hepatoprotective, antiallergic, antiulcer and antimicrobial activities. They have also been shown to exert an antiparasitic activity against *Trypanosoma* species and *Leishmania* species (*2*−*4*). In addition, protective effects against periodontal pathogens, antiviral activity against HIV (*2*) and an antitubercular potential against *Mycobacterium tuberculosis* (*5*) have been reported. UA and OA have been used in the treatment of kidney diseases and hypertension (*1*,*6*). UA and OA and their derivatives are also effective in inhibiting angiogenesis, invasion and metastasis of tumor cells (*2*).

Cells that have undergone apoptosis are rapidly removed by phagocytotic cells to maintain cellular homeostasis without damage to surrounding cells and tissue. Cells that die due to apoptosis exhibit typical morphological features such as loss of cell volume, membrane blebbing, nuclear condensation and distinct molecular changes including activation of a conserved family of proteases called caspases (*7*). Two general pathways for apoptotic cell death have been characterized, including the intrinsic and extrinsic pathways (*8*). Of note, both of the pathways begin with activation of the downstream effector caspase-3, which cleaves intracellular proteins to induce cell death (*9*). In the intrinsic pathway, damage signals are relayed to the mitochondria where commitment to apoptosis follows increased permeability of the outer and inner mitochondrial membranes. Mitochondrial permeability is mediated by interactions between antiapoptotic and proapoptotic proteins and release of cytochrome *c* into the cytosol where it activates the apoptosome complex and induces a caspase cascade that dismantles the cell.

The inhibitors of apoptosis proteins (IAPs) were first described in baculovirus, where their role is to block the apoptotic response that is initiated as a defense mechanism against viral infection (*10*). IAPs block cell death through inhibition of effector caspases and also modulate cell division, cell cycle and signal transduction. Additionally, IAPs can allow cancer cells to escape apoptotic death even in the presence of extrinsic and intrinsic stimuli. Human IAPs include c-IAP-1, c-IAP-2, XIAP (X-linked inhibitors of apoptosis protein), survivin and other members that have been described more recently (*11*). XIAP is expressed in normal tissue and is overexpressed in many cancer cell lines and cancer

*Author to whom correspondence should be addressed. Tel: 886-4-2287-9755. Fax: 886-4-2285-4378. E-mail: gcyen@nchu.edu.tw.

 Published on Web 04/23/2010

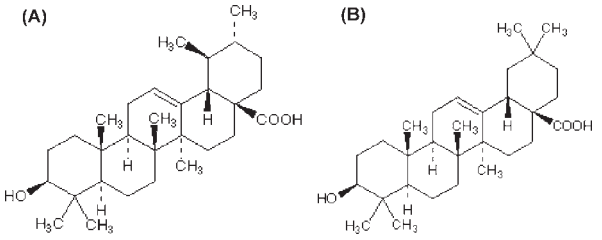

Figure 1. The structures of the isomeric triterpenoids, ursolic acid (UA) (**A**) and oleanic acid (OA) (**B**).

tissue, including ovarian, lung, pancreas, gastric, colon, liver and prostate cancer (*12*, *13*). XIAP is the most potent member of the IAP gene family in terms of its ability to inhibit caspase-3, -7 and -9, and to suppress apoptosis (*14*). The studies on IAPs in human hepatocellular carcinoma (HCC) have focused mainly on either survivin or XIAP. Expression of these IAPs in HCC is associated with a more unfavorable prognosis (*15*).

HCC is the fifth most frequent form of cancer and the third most common cause of cancer-related death worldwide (*16*). Surgical resection has been considered the optimal treatment approach, but only a small proportion of patients qualify for surgery. Furthermore, there is a high rate of recurrence after surgery. Approaches used to prevent recurrence have included chemoembolization before surgery and neoadjuvant therapy after surgery, neither of which has proved to be beneficial (*17*). Therefore, new therapeutic options are needed for more effective treatment of this malignancy. In the present study, we investigated the effects of OA and UA on cell apoptosis in human hepatocellular carcinoma HuH7 cells and the mechanisms through which these compounds function. The apoptotic effects of OA and UA on mitochondria-mediated pathways and regulation of XIAP in HuH7 cells were investigated.

MATERIALS AND METHODS

Materials. 3-(4,5-Dimethylthiazol-2-yl)-2,5-diphenyl tetrazolium bromide (MTT dye), anti-β-actin antibody, propidium iodide (PI), sodium bicarbonate, oleanolic acid (OA) and ursolic acid (UA) were purchased from Sigma Chemical Co. (St. Louis, MO). Dulbecco's modified Eagle's medium, nonessential amino acid (NEAA), sodium pyruvate, trypsin−EDTA and penicillin−streptomycin (PS) were obtained from Invitrogen Co. (Carlsbad, CA). Anti-Bax, anti-Bcl-2, anti-caspase-3, anti-caspase-9, anti-cytochrome *c* and anti-PARP [poly (ADP-ribose) polymerase] antibodies were obtained from Cell Signaling Technology (Beverly, MA). Polyvinyldifluoride (PVDF) membrane was obtained from Millipore (Bedford, MA). Fetal bovine serum (FBS) was obtained from Biological Industries Co. (Beit Haemk, Israel). Annexin V−FITC/PI assay kit, the mitochondrial permeability transition detection kit (MitoPT) and the caspase-3 fluorometric assay kit were obtained from BioVision Inc. (Mountain View, CA). The molecular mass marker for Western blotting was obtained from Pharmacia Biotech (Saclay, France).

Cell Culture. HuH7 cells were purchased from ATCC and incubated in DMEM medium supplemented with 10% (v/v) FBS, 100 units/mL penicillin, 100 μg/mL streptomycin, 1.5 g/L sodium bicarbonate, 0.1 mM NEAA and 1 mM sodium pyruvate at 37 °C in a humidified atmosphere of 95% air and 5% CO_2.

Cell Viability Assay. HuH7 cells were seeded into 24-well plates at a concentration of 5×10^4 cells/well in DMEM medium (10% FBS). After 24 h of incubation, the medium was replaced with 0.5 mL containing various concentrations (0, 10, 25, 50, 75, and 100 μM) of OA or UA and then cells were incubated for 24 h. The final concentration of solvent was less than 0.1% in the cell culture medium. Control cells were treated with 0.1% DMSO alone. After 24 h of incubation, the medium was replaced with MTT (final concentration of 0.5 mg/mL) in serum-free medium, and a further 2 h incubation followed. The MTT formazan product was dissolved in DMSO, and the optical density was measured at a wavelength of 570 nm by FLUOstar galaxy spectrophotometer (BMG Labtechnologies, Offenburg, Germany). The percent viability of the treated cells was calculated as follows: $Abs_{570nm[treatedcell]}/Abs_{570nm[control]} \times 100$. The IC_{50} value was calculated as the concentration at which the cell viability was half that of untreated controls.

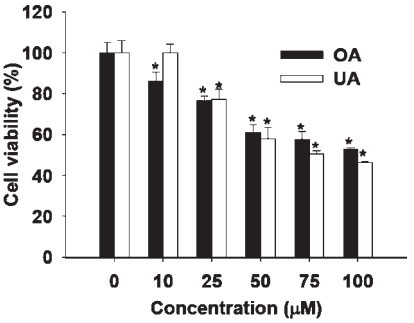

Figure 2. Effects of OA and UA on cell viability (%) in human hepatoma HuH7 cells. Cells were treated with various concentrations (0, 10, 20, 40, 60, and 80 μM) of OA or UA for 24 h. Values are means ± SD ($n = 4$). *, $p < 0.05$, compared to control group.

Cell Apoptosis Analysis by PI Staining. Cells were treated with various concentrations (0, 10, 25, 50, and 100 μM) of OA or UA for 24 h. The cells were then harvested with a trypsin−EDTA (TE) solution (0.05% trypsin and 0.02% EDTA in PBS), washed twice with PBS and fixed in 80% ethanol for 30 min at 4 °C. Fixation was followed by incubation with RNase (100 μg/mL) for 30 min at 37 °C. The cells were then stained with PI (40 μg/mL) for 15 min at room temperature in the dark and subjected to a flow cytometric analysis of DNA content using a FACScan flow cytometer (Becton-Dickinson Immunocytometery Systems, San Jose, CA). Approximately 10,000 cells were made for each sample. The percentage of cells undergoing apoptosis was calculated using CELL Quest software.

Annexin V−FITC/PI Double Staining Assay. Cells (1×10^6 cells/6 cm dish) were treated with various concentrations (0, 10, 25, 50, and 100 μM) of each chemical for 24 h at 37 °C. The cells were collected by centrifugation and stained for 10 min at room temperature with Annexin V−FITC/PI double staining of the cells was performed with the Annexin V−FITC kit (ANNEX100F, SEROTEC, U.K.). The cells were then analyzed by the FACScan flow cytometer (Becton-Dickinson Immunocytometery Systems, San Jose, CA). Annexin V−FITC and PI emissions were detected using emission filters of 525 and 575 nm, respectively. Approximately 10,000 counts were made for each sample.

Mitochondrial Membrane Potential ($\Delta\psi_m$) Analysis. Cells were seeded into a 12-well plate at a concentration of 1×10^5 cells/well in DMEM medium (10% FBS). After 24 h of incubation, the cells were treated with OA or UA (20 μM) for 3, 6, 9, 12, and 18 h. The passage of cells included rinsing once with PBS in a 12-well plate, harvesting the cells with 0.1 mL of TE solution, adding 1 mL of fresh culture medium and thoroughly dispersing the cells. Then, the mitochondrial membrane potential ($\Delta\psi_m$) was determined by using the Mito^{PT} kit (BioVision, Mountain View, CA) according to the manufacturer's protocol. Cells were resuspended in an adequate volume of the same solution and then analyzed using the FLUOstar galaxy fluorescence plate reader with an excitation wavelength of 485 nm and an emission wavelength of 520 nm for red fluorescence. The percentage (%) of $\Delta\psi_m$ value could be determined by comparing with the level of the control group.

Measurement of Caspase-3 Activity. The cells were collected after treatment with OA or UA (20 μM) for various time intervals. Then, the cells were washed with PBS and lysed in lysis buffer for 20 min at 4 °C. The caspase-3 activity was determined by fluorometric assay kit (BioVision, Mountain View, CA) according to the manufacturer's protocol. Fluorescence was measured using an excitation wavelength of 400 nm and an emission wavelength of 505 nm with a FLUOstar galaxy fluorescence plate reader. The percentage (%) of caspase-3 activity could be determined by comparing with the level of the control group.

Western Blotting Analysis. Cells were collected after treatment with OA or UA (20 μM) for various time intervals and then lysed in ice-cold lysis buffer. An aliquot of cell lysate (50−60 μg) was fractionated by SDS−PAGE on a 10% polyacrylamide gel and transferred to PVDF membrane. The membrane was incubation with a primary antibody,

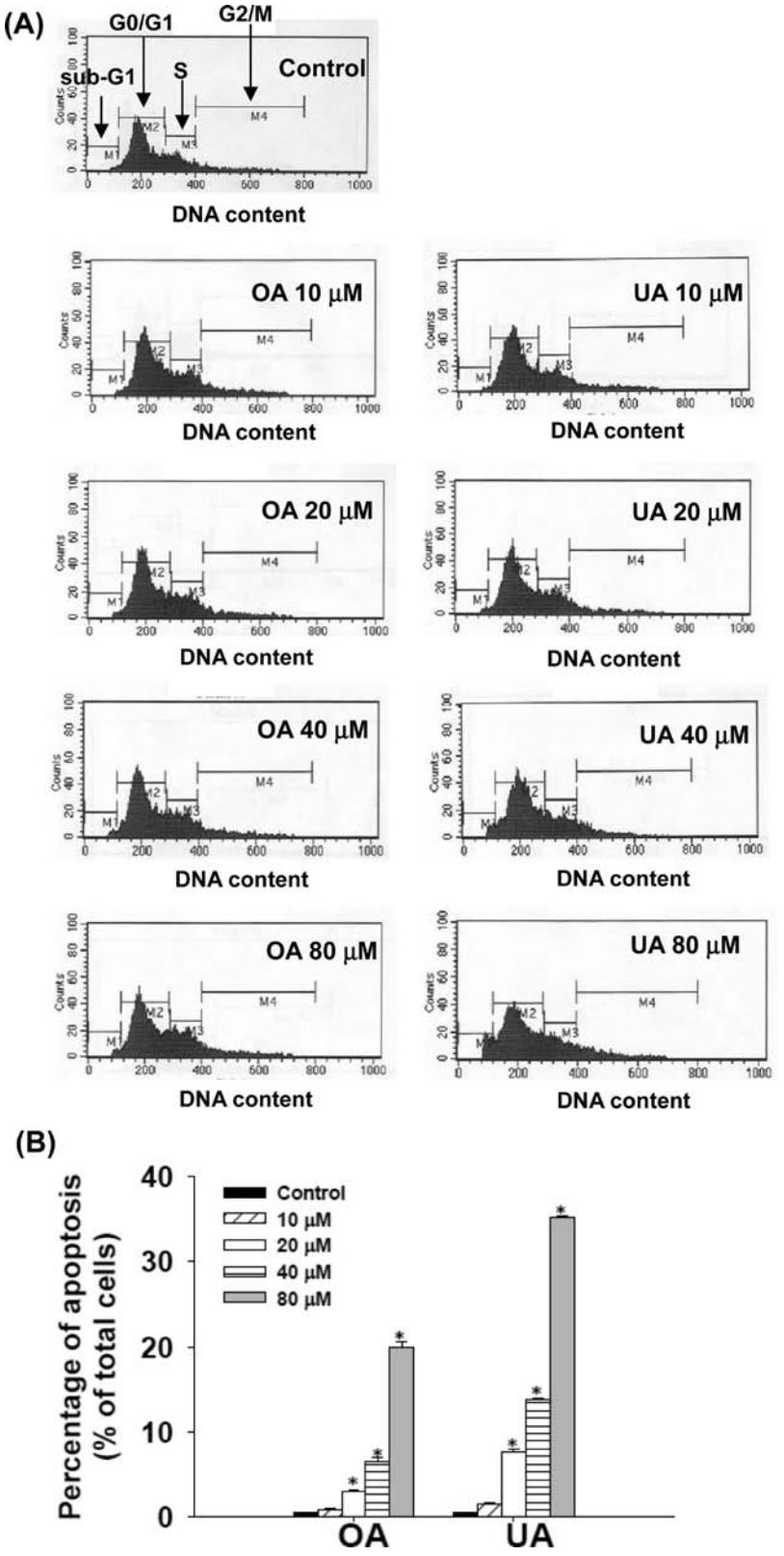

Figure 3. Effects of OA and UA on the cell cycle in human hepatoma HuH7 cells. Cells were treated with various concentrations (0, 10, 20, 40, and 80 μM) of OA or UA for 24 h. (**A**) PI stained cells were analyzed by flow cytometry. (**B**) The percentage (%) of apoptotic human hepatoma HuH7 cells treated with OA or UA. The percentage (%) of apoptotic cells was calculated with CELL Quest software (means $\pm$ SD, $n = 3$). *, $p < 0.05$ compared with control group.

washing with TBST, and then incubated with secondary antibody. Finally, antibody binding was visualized using the ECL system (Amersham-Pharmacia Biotech, Arlington Heights, IL). The expression of protein was quantified densitometrically using LabWorks 4.5 software and changes in expression were normalized to the β-actin controls.

RNA Extraction and Real-Time RT-PCR. Real-time RT-PCR was performed to determine the level of XIAP in HuH7 cells. Total RNA from HuH7 cells was isolated using the TRIzol RNA isolation kit (Life Technologies, Rockville, MD) as described in the manufacturer's manual. The cDNA was synthesized from total RNA (200 ng) by reverse

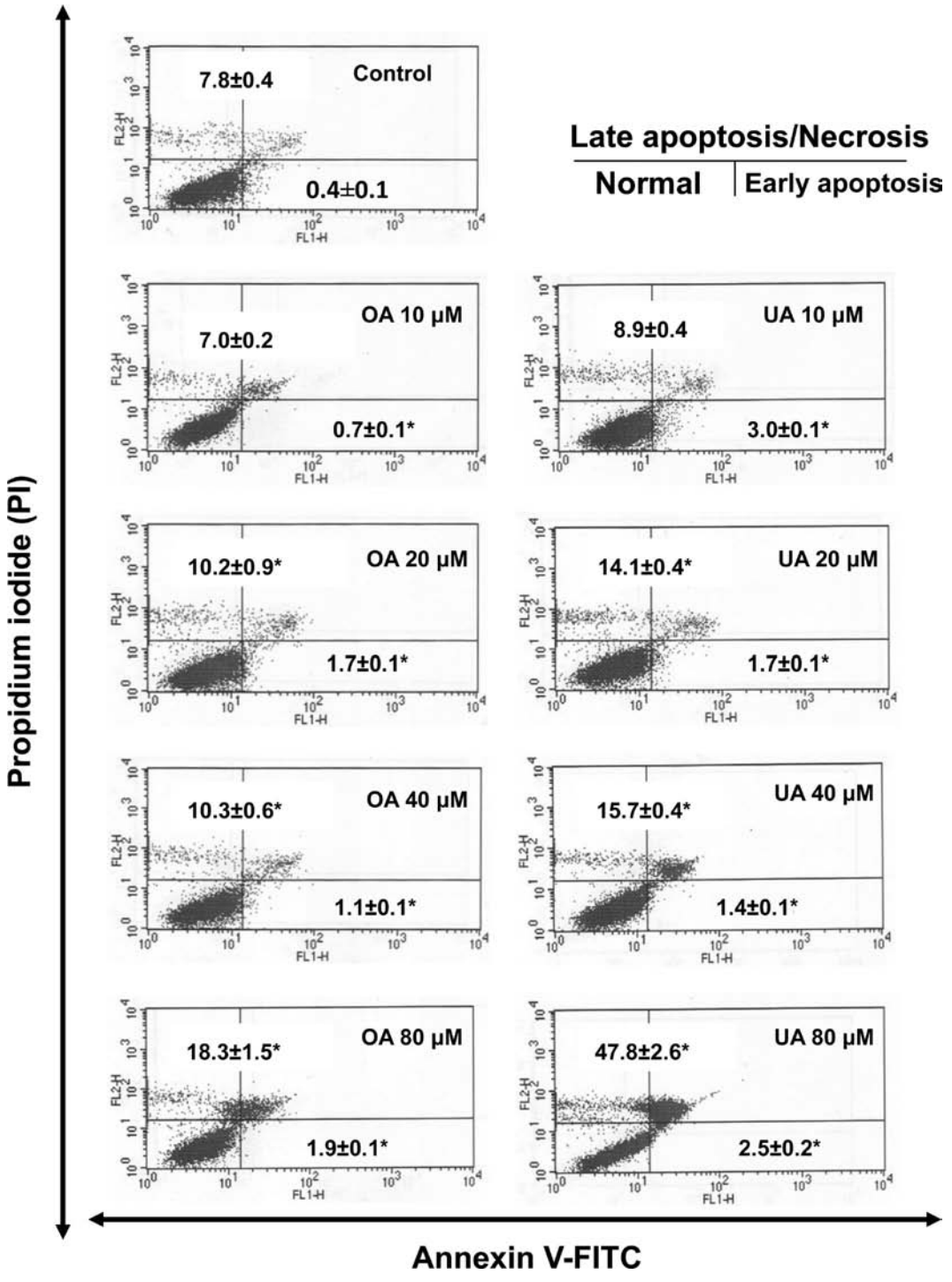

Figure 4. Effects of OA and UA on apoptosis and necrosis in human hepatoma HuH7 cells. Cells were treated with various concentrations (0, 10, 20, 40, and 80 μM) of OA or UA for 24 h and stained with Annexin−FITC/PI double stain. The percentage (%) of apoptotic and necrotic cells was calculated with CELL Quest software (means ± SD, $n = 3$). *, $p < 0.05$ compared with control group.

transcription PCR using a high-capacity cDNA reverse transcription kit (Applied Biosystems, Foster City, CA) according to the manufacturer's instructions. The following primer pairs were used: XIAP 5′-TGCCTTT-CCTGCTACATTTGG-3′ (forward) and 5′- ACACAGGGCCAAAT-CACATT-3′ (reverse); GAPDH, 5′- GGAGCCAAACGGGTCATCA-3′ (forward) and 5′- TGCAGGATGCATTGCTGACA-3′ (reverse). Relative real-time RT-PCR for detection of gene expression levels was carried out using an ABI 7300 real-time PCR system (Applied Biosystems, Foster City, CA). The reaction mixture (total volume 25 μL) contained 1× power SYBR green PCR master mix, 300 nM forward primer, 300 nM reverse primer, cDNA and DEPC-H_2O as well as commercial reagents (Applied Biosystems, Foster City, CA). The thermal profile was established according to the manufacturer's protocol. Briefly, this profile was 95 °C for 10 min to activate the enzyme followed by denaturation at 95 °C for 15 s and annealing and elongation at 60 °C for 1 min with a total of 40 cycles. Relative levels of gene expression were quantified using the ΔΔCt method, which results in a ratio of target gene expression to equally expressed housekeeping genes.

Measurement of NFκB (p65) Activity. Cells were collected after treatment with 20 μM of the chemical for various time intervals and lysed in ice-cold lysis buffer. The NFκB (p65) activity was using the 11 μL of the lysate and the AlphaScreen SureFire NFκB p65 (S536) Assay Kit (PerkinElmer, Waltham, MA) according to the manufacturer's protocol. Finally, these data were read on an AlphaScreen compatible plate reader.

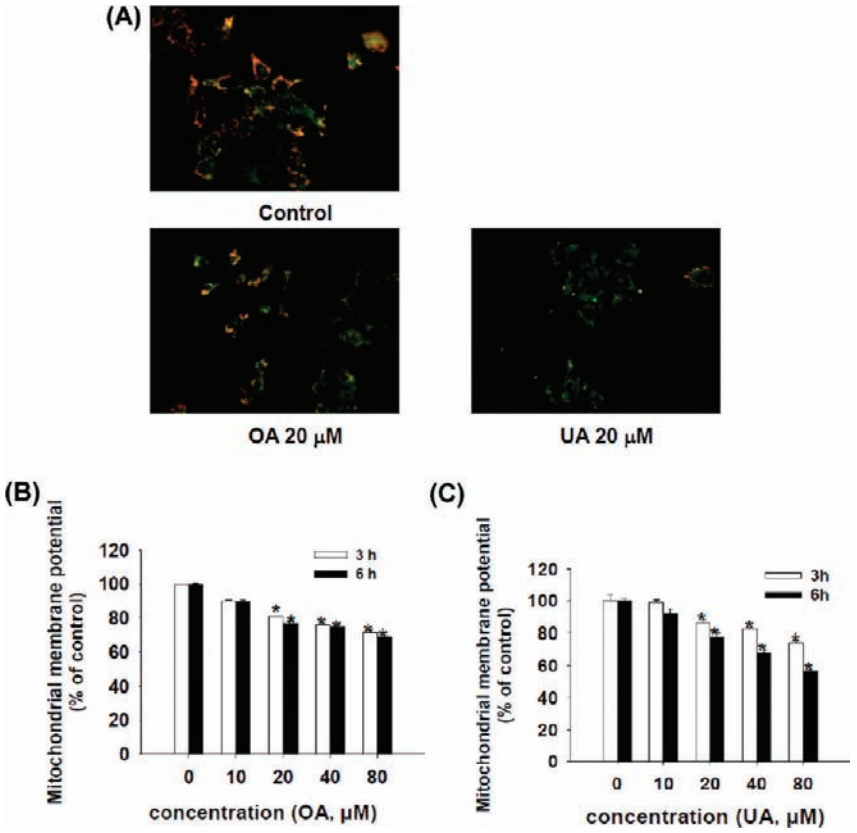

Figure 5. Effects of OA and UA on morphological changes and mitochondrial membrane potential ($\Delta\psi_m$) in human hepatoma HuH7 cells. Cells were treated with 0−80 μM OA or UA for 3 and 6 h. (**A**) Morphological changes of the cells at 6 h. (**B**) and (**C**) Percentages of mitochondrial membrane potential. Data are expressed as means ± SD (n = 3). *, $p < 0.05$ compared with control group.

The percentage (%) of NFκB (p65) activity could be determined by comparing with the level of the control group.

Statistical Analysis. Data are expressed as mean ± SD for three different determinations. Statistical significance was analyzed by one-way analysis of variance and Duncan's multiple range tests. $P < 0.05$ was defined as statistically significant.

RESULTS

Effects of OA and UA on the Viability of Human Hepatocellular Carcinoma HuH7 Cells. The inhibitory effects of OA and UA on HuH7 cell population growth were determined using the MTT assay. As shown in **Figure 2**, OA and UA (20−100 μM) progressively decreased the viability of HuH7 cells. The IC_{50} (the dose that inhibits 50% of cell population growth) values for OA and UA were 100 and 75 μM, respectively.

Effects of OA and UA on Cell Cycle Arrest and Apoptosis in HuH7 Cells. The decrease of cell viability might be caused by cell cycle arrest or apoptosis. The cell cycle and apoptosis in HuH7 cells were analyzed by flow cytometry measurements after treatment with 0−80 μM OA or UA for 24 h. The cell cycle was divided into the phases of sub-G1(M1), G1/G0 (M2), S (M3) and G2/M (M4) by flow cytometry, but cells found in the sub-G1 phase were considered to be apoptotic and necrotic due to the decrease in DNA content. As shown in **Figure 3A**, OA or UA did not cause cell cycle arrest in HuH7 cells. However, treatment of HuH7 cells with OA or UA progressively increased the values of cell counts in sub-G1 (M1) phase (**Figure 3A**). The data also indicate that OA and UA (20−80 μM) increased the percentage of apoptotic cells in a dose-dependent manner (**Figure 3B**).

Effects of OA and UA on Cell Apoptosis and Necrosis of Human Hepatoma HuH7 Cells. To further evaluate the modes of cell death (apoptosis or necrosis) induced by these compounds, HuH7 cells were treated with different concentrations of OA or UA for 24 h. Afterward, the cells were stained with Annexin V−FITC/PI and analyzed by flow cytometry. The Annexin V−FITC$^-$/PI$^-$ population was considered as normal, while Annexin V−FITC$^+$/PI$^-$, Annexin V−FITC$^+$/PI$^+$, and Annexin V−FITC$^-$/PI$^+$ populations were taken as determinations of normal, early apoptotic, late apoptotic, and necrotic cells, respectively. As shown in **Figure 4**, OA and UA at 20 μM could induce significantly ($p < 0.05$) cell death (viable cells ~17.1% and 10.2% of total cells) for 24 h, and both of these two compounds increase HuH7 cell death in a dose-dependent manner ($p < 0.05$). These data indicate that OA and UA mainly induce HuH7 cell apoptosis.

OA and UA Induce Apoptosis via a Mitochondria-Mediated Pathway. Apoptosis mediated by mitochondria is the best known intrinsic apoptosis pathway (*8*). The increased permeability of the transition pore is an important step in the induction of apoptosis by this mechanism. With respect to cell morphology, nonapoptotic cells with healthy mitochondria show red fluorescence under JC-1 fluorescence, whereas apoptotic cells show green fluorescence. As shown in **Figure 5A**, HuH7 cells showed a decrease in red fluorescence intensity when treated with 20 μM OA or UA for 6 h. Treatment with OA or UA (20−80 μM) significantly ($p < 0.05$) decreased the mitochondrial membrane potential in HuH7 cells at 3 or 6 h (**Figures 5B** and **5C**).

Bax and Bcl-2 belong to the Bcl-2 family and serve as pro- and antiapoptotic effectors, respectively. In addition, they also regulate mitochondrial outer membrane permeabilization (MOMP). The imbalance of anti- and proapoptotic protein expression is one of the major mechanisms underlying the ultimate fate of cells with respect to apoptosis. The effects of OA and UA on the constitutive levels of Bax and Bcl-2 in HuH7 cells are shown in **Figures 6A** and **6B**. In comparison with the control cells, OA and UA

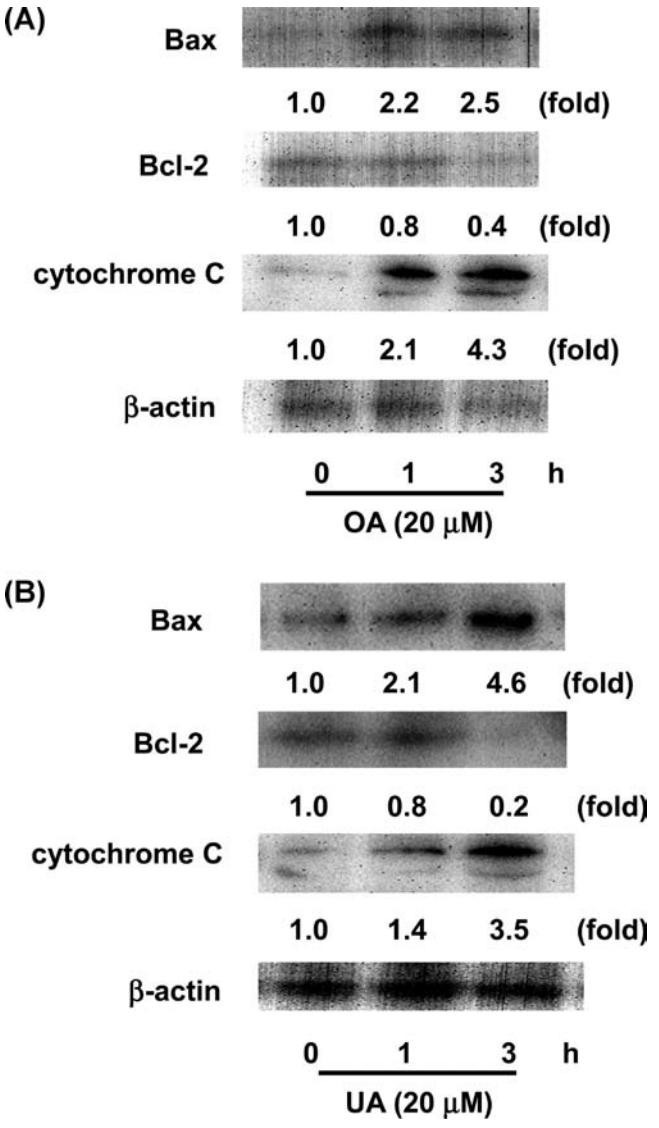

Figure 6. Effects of OA (**A**) and UA (**B**) on protein expression of Bax, Bcl-2 and cytochrome *c* in human hepatoma HuH7 cells. Cells were treated with 20 μM OA or UA for 0−6 h. The relative expression of each protein was quantified densitometrically using the LabWork 4.5 software and calculated according to β-actin reference bands.

(20 μM, 3 h) caused a significant ($p < 0.05$) increase in Bax expression by 2.5- and 4.6-fold, respectively; OA and UA (20 μM, 3 h) markedly ($p < 0.05$) decreased Bcl-2 expression by 0.4- and 0.2-fold, respectively. The data indicate that treatment with OA or UA (20 μM) could shift the ratio of Bax to Bcl-2 and lead to collapse of the mitochondrial membrane potential.

After loss of MOMP, cytochrome *c* is released into the cytosol leading to activation of the apoptosome complex and a caspase cascade. Therefore, we next investigated cytochrome *c* release in the cytosolic fraction following OA or UA treatment. OA or UA (20 μM, 3 h) treatment resulted in a significant increase in cytosolic cytochrome *c* expression by 4.3- and 3.5-fold, respectively, as compared to control cells (**Figures 6A** and **6B**). The data indicate that OA and UA could regulate apoptosis of HuH7 cells through a mitochondria-mediated pathway.

Caspase-9 is activated by cytochrome *c* early during the apoptotic process. The active caspase-9 then stimulates the proteolytic activity of other downstream caspases including that of caspase-3. Caspase-3 activation leads to the cleavage of numerous proteins including poly(ADP-ribose) polymerase (PARP). The effects of OA and UA on the time course of caspase-9, caspase-3 and PARP expression in HuH7 cells are shown in **Figures 7A** and **7B**. Exposure of HuH7 cells to OA or UA (20 μM at 24 h) caused the fragmentation of caspase-9 to increase by 1.5- and 2.7-fold, respectively, as compared with control cells. The expression of caspase-3 in OA and UA treated HuH7 cells also significantly increased by 2.0- and 2.7-fold, respectively, as compared to control cells. OA and UA treatment increased PARP cleavage by 2.2- and 2.4-fold, respectively, as compared with control cells. Additionally, treatment of cells with OA or UA for 6−18 h caused a significant ($p < 0.05$) increase in caspase-3 activity (**Figure 7C**). Exposure of HuH7 cells to OA or UA for 24 h increased the activity of caspase-3 by 136 and 138%, respectively, as compared with control cells (data not shown). These observations suggest that OA and UA might exert proapoptotic effects through a mitochondrial-mediated pathway and caspase cascade.

OA and UA Suppress Expression of XIAP mRNA. XIAP suppresses regulation of apoptosis by caspase-3, -7, and -9 (*14*). However, it is also overexpressed in many cancers. The mRNA levels of XIAP in HuH7 cells treated with 20 μM of OA or UA for different time intervals (0−18 h) are shown in **Figure 8**. The results indicate that OA and UA treatment (3 h) did not inhibit expression of XIAP mRNA in HuH7 cells. However, HuH7 cells treated with OA or UA for 6−18 h showed significant ($p < 0.05$) inhibition of XIAP mRNA levels by 50%.

OA and UA Suppress the Activity of NF-κB. Activated NF-κB, indicated by phosphorylation of the p65 subunit (pp65), regulates many biological functions. Karin et al. (*18*) suggested that the inhibition of NF-κB activation could regulate cancer cell survival. In the present study, we evaluated the inhibitory effects of OA and UA on NF-κB activity. The NF-κB activity in HuH7 cells treated with 20 μM OA or UA for 0−6 h is shown in **Figure 9**. Treatment with OA or UA (20 μM at 6 h) significantly ($p < 0.05$) suppressed the level of pp65 from 1.0 to 0.21- and 0.24-fold as compared to control cells, respectively.

DISCUSSION

OA and UA are naturally occurring triterpenoids that have been used in traditional medicine for centuries as antibacterial, antifungal, and anti-inflammatory agents. Recently, attention has been highly focused on the anticancer properties of these triterpenoids, for application in cancer prevention (*19*). Previously, we showed for the first time that OA and UA inhibited migration and invasion of human breast cancer cells through Akt/mTOR and NF-κB signaling, and thus might represent a new strategy for anticancer therapy (*20*). In addition, UA and OA were shown to induce apoptosis in HL-60 leukemia cells, B16F-10 melanoma cells, MCF-7 breast cancer cells and DU145 prostate cancer cells (*21*−*24*). Further, administration of OA and UA could efficiently inhibit hepatic stellate cell activation and provide protection against liver fibrosis in rats (*25*). Since OA and UA are relatively nontoxic to normal cells (*26*), an important implication of these findings is that these agents might play a useful role in the treatment of cancer. However, little is known regarding the proapoptotic effects of OA and UA as well as their underlying mechanisms on hepatic carcinoma. Therefore, the purpose of this study was to examine the effects of OA and UA on cell apoptosis in human hepatocellular carcinoma HuH7 cells and the mechanisms through which these compounds function. In the present study, we compared the ability of OA and UA to induce apoptosis in human hepatoma HuH7 cells. We found that OA and UA significantly decreased ($p < 0.05$) the population growth of HuH7 cells at 24 h (**Figure 2**). Cipak et al. (*27*) suggested that OA and UA could inhibit the growth of HL60 leukemia cells

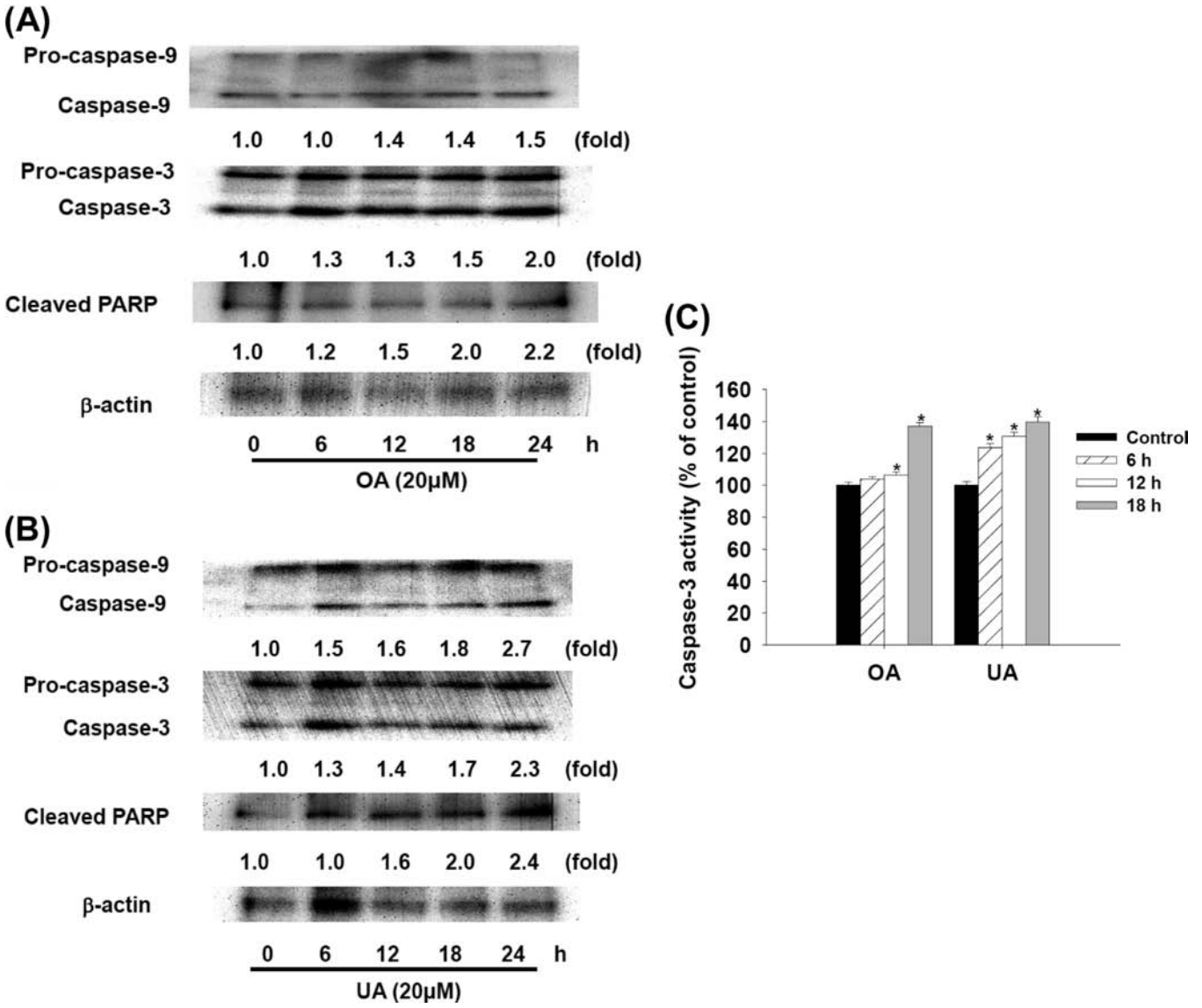

Figure 7. Effects of OA and UA on activation of caspase-3, -9 and cleavage of PARP in HuH7 cells. Protein expression of caspases and cleavage of PARP induced by 20 μM of OA (**A**) or UA (**B**) for 0−24 h. (**C**) Cytosolic fraction of cells was analyzed for caspase-3 activity treated with OA or UA. The relative expression of protein was quantified densitometrically using the LabWork 4.5 software and calculated according to β-actin reference bands.

and that they have IC_{50} values of 70 and 10 μM, respectively. Li et al. (*28*) indicated that the IC_{50} values of UA and OA on HCT15 human colon carcinoma cells are 30 and 60 μM, respectively. OA and UA have similar molecular structures but have different sites of methyl group on ring E: if the methyl group at C19 of UA is moved to C20, it changes to OA (*29*). In the present study, ursolic acid but not oleanolic acid has offered a remarkable anti-invasive activity against invasive human breast MDAMB231 cells. Since both the compounds are regioisomers, the difference in their potency may be attributed to their structural arrangement of the substituent (*30*). It is therefore speculated that the methyl group at C19 of UA is crucial for evoking HuH7 cell apoptosis. Zhang et al. (*21*) also demonstrated that OA increases the sub-G1 phase and affected the cell cycle in HL-60 cells. These studies indicate that OA and UA have high cytotoxicity and induce apoptosis in cancer cells.

Mitochondria play an essential role in cell death signal transduction. Increasing the membrane permeability and collapsing the mitochondrial membrane potential results in the rapid release of caspase activators, such as cytochrome *c*, into the cytoplasm (*31*). In general, a change in the externalization of membrane phosphatidylserine (PS) follows the reduction of mitochondrial membrane potential (*32*). Detection of the mitochondrial membrane potential provides an early indication of the initiation of cellular apoptosis. In the present study, treatment of HuH7 cells with OA and UA caused mitochondrial membrane potential collapse (**Figure 5**).

The proteins of the Bcl-2 family form ion channels in biological membranes. These channels regulate apoptosis by influencing the permeability of the intracellular membrane of mitochondria. The Bcl-2 family includes both antiapoptotic members, such as Bcl-2 and Bcl-xL, and proapoptotic members, such as Bax, Bad and Bak. It has been proposed that the ratio between Bcl-2 and Bax is more important in the regulation of apoptosis than the level of each Bcl-2 family protein separately. Furthermore, Bax overexpression alone has been demonstrated to accelerate apoptotic cell death (*33*). UA was able to downregulate Bcl-2 protein levels to induce breast cancer MCF-7 cells (*23*). Zhang et al. (*24*) reported that UA causes phosphorylation of Bcl-2 to mediate Bcl-2 inactivation and degradation in DU145 cells. UA also suppresses the ability of NF-κB to mediate activation of Bcl-2 in B16F-10 melanoma cells (*22*). Our data indicate that the

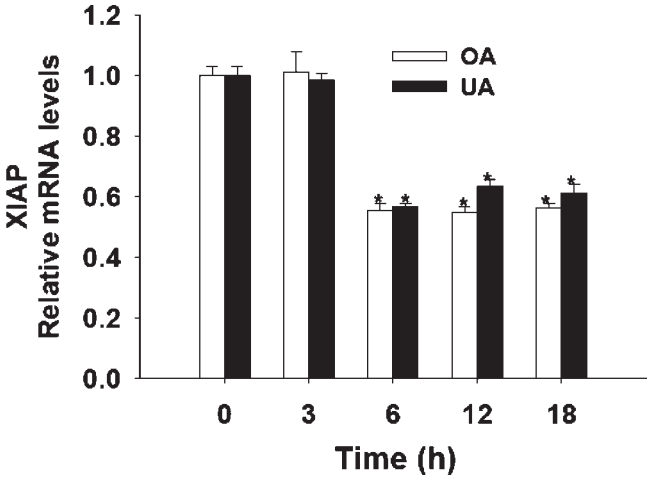

Figure 8. Effects of OA and UA on expression of XIAP mRNA in human hepatoma HuH7 cells. Cells were treated with 20 μM of OA or UA for 0−18 h. Data are expressed as means ± SD (n = 3). *, $p < 0.05$ compared with control group.

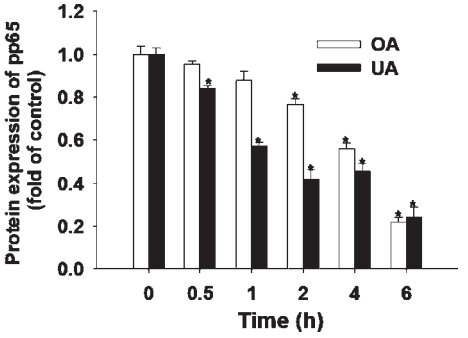

Figure 9. Effects of OA and UA on activity of NF-κB (p65) in human hepatoma HuH7 Cells. Cells were treated with 20 μM of OA or UA for 0−6 h. Data are expressed as means ± SD (n = 3). *, $p < 0.05$ compared with control group.

expression levels of pro- and antiapoptotic Bcl-2 family members were altered by OA and UA treatments followed by the release of mitochondrial cytochrome c into the cytosol (**Figure 6**). One possibility is that the protein levels of antiapoptotic Bcl-2 decreased and proapoptotic Bax increased upon treatment with OA and UA. However, this change in protein levels might play a key role in OA and UA induced apoptosis in HuH7 cells.

It is well-known that proteins of the Bcl-2 family play a pivotal role in apoptosis by interfering with caspases, which are the key effectors of programmed cell death. The caspase cascade is initiated by the proteolysis of inactive procaspases, and it is propagated by the cleavage of downstream caspases and substrates such as PARP [poly(ADP-ribose)polymerase cleavage] (*33*). Caspase-9 is a member of the CED-3 family and bears high similarity to caspase-3. Therefore, caspase-3 is one of the key mediators of apoptosis. Andersson et al. (*34*) indicated that UA acts in a dose-dependent manner and results in activation of caspase-3, -8, and -9 in HT29 cells. Zhang et al. (*21*) also reported that OA induces apoptosis in HL-60 cells through caspase-3 and -9 activation and PARP cleavage. In the present study, the results showed that OA- and UA-induced apoptosis were controlled through activation of caspase-3 and -9 (**Figures 7A** and **7B**). Furthermore, our data also indicate that OA and UA enhanced caspase-3 activity in HuH7 cells (**Figure 7C**). Cleavage of procaspase-3 by caspase-9 produces an active enzyme that is capable of cleaving PARP. PARP is a

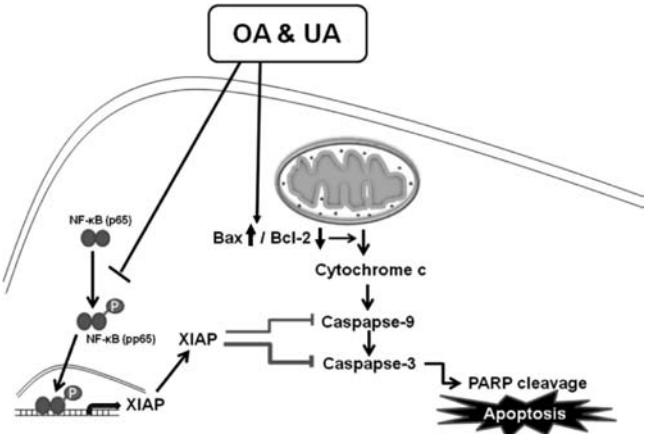

Figure 10. Schematic representation of the mechanism by which OA and UA induce apoptosis in human hepatoma HuH7 cells. OA and UA can mediate the apoptotic pathway through the induction of stress proteins. OA and UA lead to loss of the mitochondrial transmembrane potential ($\Delta\psi_m$), release of cytochrome c from the mitochondria into the cytosol and subsequent activation of caspase-9 and caspase-3, followed by the cleavage of PARP. The ratio of expression levels of pro- and antiapoptotic Bcl-2 family members is also changed by OA and UA treatment. OA and UA inhibit expression of the XIAP gene through suppression of NF-κB (p65) activity.

chromatin-bound enzyme that is activated by DNA strand breaks and catalyzes the successive transfer of ADP-ribose units from NAD to nuclear proteins. Cleavage of PARP results in its inactivation, slowing the DNA repair process and enhancing the apoptotic process. We also indicated that OA and UA induced the cleavage of PARP and promoted apoptosis in HuH7 cells (**Figures 7A** and **7B**).

Both XIAP and cIAP-1 levels are elevated in cancer cells. These proteins also correlate with the acquired drug resistance phenotype and cell survival. In the present study, we found that OA or UA treatment could inhibit expression of XIAP mRNA (**Figure 8**). Tang et al. (*35*) reported that the expression of survivin, which is other IAP protein, could be downregulated by UA in HepG2 cells. The typical NF-κB is a heterodimer composed of p52 and p65 subunits, which are the most frequent components of active NF-κB. NF-κB acts in an intrinsic fashion to confer resistance to cell death by activating the expression of antiapoptotic genes in many human tumors. Karin (*18*) suggested that NF-κB modulates other genes associated with cell cycle regulation or the cell survival pathway. Moreover, the NF-κB transcription factor family also controls the expression of antiapoptotic genes that are members of the Bcl-2 and c-IAP families (*18*). In addition, Shishodia (*36*) suggested that UA suppresses NF-κB activation and downregulates downstream protein expression. Our results demonstrate that OA and UA decreased the phosphorylation of NF-κB subunit (pp65). Mayo et al. (*37*) suggested that the transcription factor NF-κB family regulates the expression of antiapoptotic genes, which including Bcl-2 and IAP families. In addtion, XIAP has been found to be a potent but restricted inhibitor targeting caspase-3, -7 and -9, which are capable of selectively blocking apoptosis (*14*). In the present study, we demonstrated that the expression of XIAP mRNA could be modulated by OA and UA treatment (**Figure 9**). Thus, OA- and UA-induced HuH7 cell apoptosis might decrease the activation of NF-κB and its downstream Bcl-2 and IAP proteins which are associated with the mitochondria-dependent apoptotic pathway.

In conclusion, the present results show that OA and UA lead to loss of the mitochondrial transmembrane potential, regulation of

Bcl-2 family members, release of cytochrome *c* from the mitochondria into the cytosol and subsequent activation of caspase-9 and caspase-3, followed by cleavage of PARP and induction of apoptosis in HuH7 cells. In addition, OA and UA also suppressed the activity of NF-κB and modulated the expression of XIAP mRNA to influence cancer cell survival (**Figure 10**). Based on the results of this study, we propose that OA- and UA-enriched plants should be further tested to determine whether they are effective for prevention of human cancer in an *in vivo* model.

LITERATURE CITED

(1) Somova, L. I.; Shode, F. O.; Mipando, M. Cardiotonic and antidysrhythmic effects of oleanolic and ursolic acids, methyl maslinate and uvaol. *Phytomedicine* **2004**, *11*, 121–129.

(2) Kowalski, R. Studies of selected plant raw materials as alternative sources of triterpenes of oleanolic and ursolic acid types. *J. Agric. Food Chem.* **2007**, *55*, 656–662.

(3) Cunha, W. R.; Martins, C.; Da Silva Ferreira, D.; Crotti, A. E.; Lopes, N. P.; Albuquerque, S. In vitro trypanocidal activity of triterpenes from *Miconia* species. *Planta Med.* **2003**, *69*, 470–472.

(4) Torres-Santos, E. C.; Lopes, D.; Oliveira, R. R.; Carauta, J. P.; Falcao, C. A.; Kaplan, M. A.; Rossi-Bergmann, B. Antileishmanial activity of isolated triterpenoids from *Pourouma guianensis*. *Phytomedicine* **2004**, *11*, 114–120.

(5) Gua, J. Q.; Wang, Y.; Franzblau, S. G.; Montenegro, G.; Timmermann, B. N. Constituents of *Quinchamalium majus* with potential antitubercular activity. *Z. Naturforsch. C* **2004**, *59*, 797–802.

(6) Yoshimura, H.; Sugawara, K.; Saito, M.; Murakami, S.; Miyata, N.; Kawashima, A.; Morimoto, S.; Gao, N.; Zhang, X.; Yang, J. *In vitro* TGF-beta1 antagonistic activity of ursolic and oleanolic acids isolated from *Clerodendranthus spicatus*. *Planta Med.* **2003**, *69*, 673–675.

(7) Johnstone, R. W.; Ruefli, A. A.; Lowe, S. W. Apoptosis: A link between cancer genetics and chemotherapy. *Cell* **2002**, *108*, 153–164.

(8) Alvarez, S.; Drane, P.; Meiller, A.; Bras, M.; Deguin-Chambon, V.; Bouvard, V.; May, E. A comprehensive study of p53 transcriptional activity in thymus and spleen of γ-irradiated mouse: High sensitivity of genes involved in the two main apoptotic pathways. *Int. J. Radiat. Biol.* **2006**, *82*, 761–770.

(9) Cohen, G. M. Caspases: the executioners of apoptosis. *Biochem. J.* **1997**, *326*, 1–16.

(10) Crook, N. E.; Clem, R. J.; Miller, L. K. An apoptosis-inhibiting baculovirus gene with a zinc finger-like motif. *J. Virol.* **1993**, *67*, 2168–2174.

(11) Liston, P.; Fong, W. G.; Korneluk, R. G. The inhibitors of apoptosis: there is more to life than Bcl2. *Oncogene* **2003**, *22*, 8568–8580.

(12) Wu, M.; Yuan, S.; Szporn, A. H.; Gan, L.; Shtilbans, V.; Burstein, D. E. Immunocytochemical detection of XIAP in body cavity effusions and washes. *Mod. Pathol.* **2005**, *18*, 1618–1622.

(13) Berezovskaya, O.; Schimmer, A. D.; Glinskii, A. B.; Pinilla, C.; Hoffman, R. M.; Reed, J. C.; Glinsky, G. V. Increased expression of apoptosis inhibitor protein XIAP contributes to anoikis resistance of circulating human prostate cancer metastasis precursor cells. *Cancer Res.* **2005**, *65*, 2378–2386.

(14) Stennicke, H. R.; Ryan, C. A.; Salvesen, G. S. Reprieval from execution: themolecular basis of caspase inhibition. *Trends Biochem. Sci.* **2002**, *27*, 94–101.

(15) Shiraki, K.; Sugimoto, K.; Yamanaka, Y.; Yamaguchi, Y.; Saitou, Y.; Ito, K.; Yamamato, N.; Yamanaka, T.; Fujikawa, K.; Murata, K.; Nakano, T. Overexpression of X-linked inhibitor of apoptosis in human hepatocellular carcinoma. *Int. J. Mol. Med.* **2003**, *12*, 705–708.

(16) Llovet, J. M.; Burroughs, A.; Bruix, J. Hepatocellular carcinoma. *Lancet* **2003**, *362*, 1907–1917.

(17) Carr, B. I. Hepatocellular carcinoma: current management and future trends. *Gastroenterology* **2004**, *127*, 218–224.

(18) Karin, M. Nuclear factor-kappa B in cancer development and progression. *Nature* **2006**, *441*, 431–436.

(19) Sogno, I.; Vannini, N.; Lorusso, G.; Cammarota; R., Noonan, D. M.; Generoso, L.; Sporn, M. B.; Albini, A. Anti-angiogenic activity of a novel class of chemopreventive compounds: oleanic acid terpenoids. *Recent Results Cancer Res. 181*, 209−212.

(20) Yeh, C. T.; Wu, C. H.; Yen, G. C. Ursolic acid, a naturally occurring triterpenoid, suppresses migration and invasion of human breast cancer cells by modulating c-Jun N-terminal kinase, Akt and mammalian target of rapamycin signaling. *Mol. Nutr. Food Res.* **2010**, DOI: 10.1002/mnfr.200900414.

(21) Zhang, P.; Li, H.; Chen, D.; Ni, J.; Kang, Y.; Wang, S. Oleanolic acid induces apoptosis in human leukemia cells through caspase activation and poly(ADP-ribose) polymerase cleavage. *Acta. Biochim. Biophys. Sin.* (*Shanghai*) **2007**, *39*, 803–809.

(22) Manu, K. A.; Kuttan, G. Ursolic acid induces apoptosis by activating p53 and caspase-3 gene expressions and suppressing NF-kappaB mediated activation of bcl-2 in B16F-10 melanoma cells. *Int. Immunopharmacol.* **2008**, *8*, 974–981.

(23) Kassi, E.; Sourlingas, T. G.; Spiliotaki, M.; Papoutsi, Z.; Pratsinis, H.; Aligiannis, N.; Moutsatsou, P. Ursolic acid triggers apoptosis and Bcl-2 downregulation in MCF-7 breast cancer cells. *Cancer Invest.* **2009**, *27*, 723–733.

(24) Zhang, Y. X.; Kong, C. Z.; Wang, H. Q.; Wang, L. H.; Xu, C. L.; Sun, Y. H. Phosphorylation of Bcl-2 and activation of caspase-3 via the c-Jun N-terminal kinase pathway in ursolic acid-induced DU145 cells apoptosis. *Biochimie* **2009**, *91*, 1173–1179.

(25) Shyu, M. H.; Kao, T. C.; Yen, G. C. Hsian-tsao (Mesona procumbens Heml.) prevents against rat liver fibrosis induced by CCl(4) via inhibition of hepatic stellate cells activation. *Food. Chem. Toxicol.* **2008**, *46*, 3707–3713.

(26) Liu, J. Pharmacology of oleanolic acid and ursolic acid. *J. Ethnopharmacol.* **1995**, *49*, 57–68.

(27) Cipak, L.; Grausova, L.; Miadokva, E.; Novotny, L.; Rauko, P. Dual activity of triterpenoids: apoptotic versus antidifferentiation effects. *Arch. Toxicol.* **2006**, *80*, 429–435.

(28) Li, J.; Guo, W. J.; Yang, Q. Y. Effects of ursolic acid and oleanolic acid on human colon carcinoma cell line HCT15. *World J. Gastroenterol.* **2002**, *8*, 493–495.

(29) Es-saady, D.; Najid, A.; Simon, A.; Denizot, Y.; Chulia, A. J.; De-lage, C. Effects of ursolic acid and its analogs on soybean 15-lipoxygenase activity and the proliferation rate of a human gastric tumor-cell line. *Mediators Inflammation* **1994**, *3*, 181–184.

(30) Ovesná, Z.; Kozics, K.; Slamenová, D. Protective effects of ursolic acid and oleanolic acid in leukemia cells. *Mutat. Res.* **2006**, *600*, 131–137.

(31) Green, D. R.; Reed, J. C. Mitochondria and apoptosis. *Science* **1998**, *281*, 1309–1312.

(32) Raghuvar Gopal, D. V.; Narkar, A. A.; Badrinath, Y.; Mishra, K. P.; Joshi, D. S. Protection of Ewing's sarcoma family tumor (ESFT) cell line SK-N-MC from betulinic acid induced apoptosis by R-DL-tocopherol. *Toxicol. Lett.* **2004**, *153*, 201–212.

(33) Hengartner, M. O. The biochemistry of apoptosis. *Nature* **2000**, *407*, 770–776.

(34) Andersson, D.; Liu, J. J.; Nilsson, A.; Duan, R. D. Ursolic acid inhibits proliferation and stimulates apoptosis in HT29 cells following activation of alkaline sphingomyelinase. *Anticancer Res.* **2003**, *23*, 3317–3322.

(35) Tang, C.; Lu, Y. H.; Xie, J. H.; Wang, F.; Zou, J. N.; Yang, J. S.; Xing, Y. Y.; Xi, T. Downregulation of survivin and activation of caspase-3 through the PI3K/Akt pathway in ursolic acid-induced HepG2 cell apoptosis. *Anticancer Drugs* **2009**, *20*, 249–258.

(36) Shishodia, S.; Majumdar, S.; Banerjee, S.; Aggarwal, B. B. Ursolic acid inhibits nuclear factor-κB activation induced by carcinogenic agents through suppression of IκBa kinase and p65 phosphorylation: correlation with down-regulation of cyclooxygenase 2, matrix metalloproteinase 9, and cyclin D1. *Cancer Res.* **2003**, *63*, 4375–4383.

(37) Mayo, M. W.; Baldwin, A. S. The transcription factor NF-κB: control of oncogenesis and cancer therapy resistance. *Biochim. Biophys. Acta* **2000**, *1470*, M55–M62.

Received for review February 10, 2010. Revised manuscript received April 3, 2010. Accepted April 12, 2010. This research work was partially supported by the National Science, Republic of China, under grant NSC98-2622-B005-010-CC2.